Insulating Josephson Junction Chains as Pinned Luttinger Liquids

Karin Cedergren,[1] Roger Ackroyd,[1] Sergey Kafanov,[1,*] Nicolas Vogt,[2] Alexander Shnirman,[3,4,5] and Timothy Duty[1,†]
[1]*Centre for Engineered Quantum Systems (EQuS), School of Physics, University of New South Wales, Sydney 2052, Australia*
[2]*Chemical and Quantum Physics, School of Science, RMIT University, Melbourne 3001, VIC 3001 Australia*
[3]*Institut für Theorie der Kondensierten Materie, Karlsruhe Institute of Technology, D-76128 Karlsruhe, Germany*
[4]*Landau Institute for Theoretical Physics, 119334 Moscow, Russia*
[5]*Institute of Nanotechnology, Karlsruhe Institute of Technology, D-76344 Eggenstein-Leopoldshafen, Germany*
(Received 24 March 2017; published 18 October 2017)

Quantum physics in one spatial dimension is remarkably rich, yet even with strong interactions and disorder, surprisingly tractable. This is due to the fact that the low-energy physics of nearly all one-dimensional systems can be cast in terms of the Luttinger liquid, a key concept that parallels that of the Fermi liquid in higher dimensions. Although there have been many theoretical proposals to use linear chains and ladders of Josephson junctions to create novel quantum phases and devices, only modest progress has been made experimentally. One major roadblock has been understanding the role of disorder in such systems. We present experimental results that establish the insulating state of linear chains of submicron Josephson junctions as Luttinger liquids pinned by random offset charges, providing a one-dimensional implementation of the Bose glass, strongly validating the quantum many-body theory of one-dimensional disordered systems. The ubiquity of such an electronic glass in Josephson-junction chains has important implications for their proposed use as a fundamental current standard, which is based on synchronization of coherent tunneling of flux quanta (quantum phase slips).

DOI: 10.1103/PhysRevLett.119.167701

The combined effects of interaction and disorder in superfluid bosonic condensates can have drastic consequences, leading to the Mott insulator [1,2] and Bose-Anderson glass [3–5]. The latter is thought to describe helium-4 in porous media, cold atoms in disordered optical potentials, disordered magnetic insulators, and thin superconducting films. The prototypical Bose-Hubbard model without disorder predicts a Beresinskii-Kosterlitz-Thouless quantum phase transition between superfluid and Mott insulator. Experimental implementation using arrays of Josephson junctions (JJ) has been explored [6–8]; however, the possibility of the insulating glass has not been considered.

One-dimensional arrays of Josephson junctions are notable for application as a fundamental current standard [9,10], which is based on synchronization of a "dual" Josephson effect, envisioned to arise from coherent quantum tunneling of flux quanta, or so-called quantum phase slips [11–15]. Unlike the Mott insulator, the insulating glass is compressible; therefore, ac synchronization of charge may not be possible. Although the presence of offset charge disorder is well established for small superconducting islands, it has not been sufficiently addressed in regards to dual Josephson effects.

We have measured critical voltages for a large number of simple chains of submicron Josephson junctions with significantly varying energy scales. We observe universal scaling of critical voltage with single-junction Bloch bandwidth. Our measurements reveal a localization length exponent that steepens with Luttinger parameter, K, arising from precursor fluctuations as one approaches the Bose glass-superfluid quantum phase transition. This contrasts with the fixed exponent found for classical pinning of charge density waves [16], vortex lattices [17], and disordered spin systems [18], and is in excellent agreement with the quantum theory of one-dimensional disordered bosonic insulators [4,5,19]. Luttinger liquids (LLs) characteristically obey scaling laws with K-dependent exponents; thereby we demonstrate a unique signature of pinned Luttinger liquids using insulating JJ chains.

A Josephson-junction array is described by a coupled quantum rotor model, which is equivalent to a long-ranged Bose-Hubbard model with large average number of bosons $\langle n\rangle$, per site. The Josephson energy E_J is related to the hopping matrix element t of the Bose-Hubbard model as $\langle n\rangle t \to E_J$. The on-site energy U of the Bose-Hubbard model is related to the single-junction Cooper-pair charging energy, $E_{\mathrm{CP}} \equiv (2e)^2/2C_J$, where C_J is the junction capacitance. In Josephson-junction arrays, a third energy scale, $E_0 = (2e)^2/2C_0$, arises from the inevitable capacitive coupling to ground, C_0. For a one-dimensional chain with only nearest-neighbor junction capacitances C_J, and capacitances to ground, the Coulomb interaction U_{ij} decays exponentially as $U_{ij} \simeq \Lambda E_{\mathrm{CP}} \exp(-|i-j|/\Lambda)$, where the screening length Λ is given by $\Lambda = \sqrt{C_J/C_0} = \sqrt{E_0/E_{\mathrm{CP}}}$.

In the insulating state of a one-dimensional chain of junctions, it is more convenient to cast the model in terms of continuous quasicharges $\{q_i\}$, where $q_i \equiv \pi Q_i/2e$ is proportional to the charge Q_i that has flown into junction i,

rather than discrete island charges $\{n_i\}$ [20]. In this way, an effective Langrangian is obtained [22,23],

$$\mathcal{L} = \frac{1}{2\pi K}\sum_i \left[\frac{\dot{q}_i^2}{v} - v(q_i - q_{i+1})^2\right] - \sum_i \epsilon_0(q_i + f_i), \tag{1}$$

where charge velocity $v = \sqrt{2E_0E_J}/\hbar$, Luttinger parameter $K \equiv \pi\sqrt{E_J/2E_0}$, and the f_i describe random offset charges. The energy E_0 is seen to be the elastic energy for small displacements of quasicharge.

Likharev and Zorin [21] found that the energy levels for a single current-biased junction are given by periodic Bloch energy bands in quasicharge. The lowest energy band ϵ_0 is characterized by its Bloch bandwidth W. For large $g = E_J/E_{\mathrm{CP}}$, the energy bands become sinusoidal and $\epsilon_0 = -(W/2)\cos(2q)$, with

$$W = 16\sqrt{\frac{E_J E_{\mathrm{CP}}}{\pi}}(2g)^{1/4}e^{-\sqrt{32g}}, \tag{2}$$

so that in this limit, the continuum version of Eq. (1) describes a sine-Gordon model [24].

In this Letter we exploit the critical voltage as a probe of localization (pinning) length N_L, which can be determined using a generalized depinning theory. The classical limit of depinning, as applied to JJ chains, has been discussed recently by Vogt *et al.* [22]. Under the assumption of maximal offset charge disorder, with the f_i distributed independently for each site, the last term in Eq. (1) becomes random, bounded by $\pm W/2$. The quasicharge is then pinned in a manner analogous to pinning of an elastic charge density wave by random impurities [16].

Classical pinning of an elastic object by a random potential arises in many contexts, and is related to the study of interface roughness [25]. As found in the context of disorderd spin systems [18], and pinning of vortex lattices in type-II superconductors [17], one finds a characteristic length N_L over which the ground state remains ordered. N_L is set by competition between distortion of the elastic object, which lowers the total pinning energy, but simultaneously increases the elastic energy. It is found self-consistently that N_L has a characteristic power law dependence on the range of the pinning distribution, here, $N_L \propto W^{-2/3}$. The depinning force is proportional to the elastic energy, E_0, and inversely proportional to N_L^2. For chains larger than N_L, the pinning force is simply the critical voltage divided by the number of junctions in the chain, and therefore, $eV_c/N \propto E_0^{-1/3}W^{4/3}$.

One notes from Eq. (2) that the leading order prefactor of W is a constant times the junction plasma frequency, $\hbar\omega_p = \sqrt{2E_JE_{\mathrm{CP}}}$. In order to compare chain families of widely varying $\hbar\omega_p$, and chain length N, we express the critical voltage and Bloch bandwidth as dimensionless variables, $v \equiv eV_c/N\hbar\omega_p$ and $w \equiv W/\hbar\omega_p$, so that in the classical limit,

$$v = aw^{4/3}, \tag{3}$$

with the prefactor, $a = b(K/\Lambda)^{1/3}$, with b being a constant $\mathcal{O}(1)$.

Recently, voltage-biased Josephson junction arrays have been described using a dual Josephson picture, where the critical voltage arises from coherent quantum phase slips (QPS) [10,11,14,15]. The phase slip rate across each junction in the large g limit is $W/2h$, and under the assumption of independent phase slips across each junction, the critical voltage of a chain would be $V_c = N\max|d\epsilon_0(q)/dq|(\pi/2e)$, which for large g becomes $\pi NW/2e$, leading to $v = \pi w/2$, that is, an exponent of 1 rather than $\frac{4}{3}$. The simple QPS picture is thus seen to assume rigid quasicharge across the chain, and ignores offset charge disorder. The assumption of rigid quasicharge is arguably reasonable in the case of an infinite screening length Λ, or deep in the incompressible Mott insulating state, but questionable in the compressible Bose glass state.

So far we have only considered the case of classical depinning. When quantum fluctuations are included [4,5,19], one finds that the localization length increases with increasing Luttinger constant, K, such that $N_L \propto w^{-2/(3-2K)}$, which diverges at the Bose glass-superfluid (BG-SF) transition, $K_c = 3/2$. The critical voltage then scales as

$$v = aw^{\alpha}, \qquad \alpha = 4/(3-2K). \tag{4}$$

The dominant effect of quantum fluctuations of charge, $K \neq 0$, is seen to change the exponent α, as the prefactor a is only very weakly dependent on K.

We have experimentally determined the dependence of the critical voltage on chain length N, scaled Bloch bandwidth w (varying both plasma frequency ω_p and g), and screening length Λ, by fabricating and measuring a large ensemble of $\mathrm{Al/AlO}_x\mathrm{/Al}$ single-junction chains. Several families of devices with different plasma

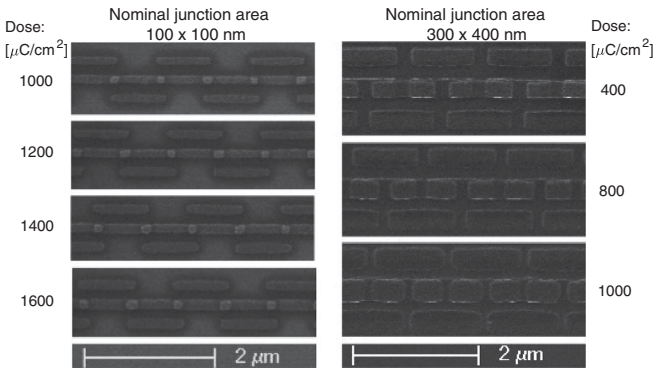

FIG. 1. Scanning electron micrograph showing two array families with high (left panel) and low (right panel) plasma frequencies, and nominal junction areas of 100×100 and 300×400 nm, respectively. The specific capacitance is 95 and 54 $\mathrm{fF}/\mu\mathrm{m}^2$, respectively. The precise junction area within a family is modulated by the exposure dose.

frequencies, controlled by the oxide barrier thickness, were initially fabricated on substrates without ground planes (see Fig. 1). Within a device family, we vary the junction area A across the family, in order to geometrically tune g [see Supplemental Material (SM) [26]].

Our approach is in contrast with previous studies, which have mostly been carried out using SQUID arrays, for which each serial element of the chain consists of two junctions in parallel forming a low inductance loop. The advantage of using such SQUID arrays is that using a single device, the effective E_J for an element can be tuned *in situ* by applying an external magnetic field. However, this simultaneously changes both g and ω_p. Instead we were motivated to examine junction chains that were as simple as possible to fabricate uniformly, not susceptible to disorder arising from unequal SQUID junctions or variations in loop areas, and unaffected by low-frequency flux noise. Furthermore, we desired to keep the plasma frequency as constant as possible for a given family of devices.

For each device, we first obtain an accurate measure of the average junction charging energy, E_{CP}, from the voltage offset, V_{off}, of each device found from extrapolating its linear current-voltage characteristic (IVC) from large voltage bias. As noted in [26–28], the experimentally determined charging energy is found as $E_{\mathrm{CP}} = 4eV_{\mathrm{off}}/N$, and the average Josephson energy E_J across the chain is found from the normal state conductance using the Abegaokar-Baratoff relation. Note that a given device can be parametrized by either E_J and E_{CP}, or alternatively $\hbar\omega_p$ and g.

Next we measure the critical voltage V_c, deep in the subgap region, $V \ll 2N\Delta/e$, where Δ is the superconducting gap. Many of the measured devices have nonhysteretic IVCs in this region. For these devices, the critical voltages are determined to be the voltage at which the current becomes measurably greater than the noise level in the zero-current region. Typically this current is 3 orders of magnitude or more greater than the zero-current noise level. Some devices with larger g exhibit hysteretic IVCs. For these, the critical voltage is found as the average of the distribution of switching voltages. The switching voltage is defined as the voltage for which the current makes a large jump (maximum dI/dV) upon stepping up from zero voltage bias, as illustrated in Fig. 2. The standard deviations of the switching voltages are at most a few percent of the distribution average critical voltage (see SM [26] for additional details).

In order to explicitly test the influence of K on the scaling of critical voltage, we also fabricated and measured a family of devices having a gold ground plane buried under 50 nm of atomic layer deposited Al_2O_3. The presence of the ground plane increases the capacitance to ground C_0, hence lowering Λ, and therefore increasing K for a given range of w, since $K = \pi\Lambda^{-1}\sqrt{g/2}$. Increased K produces a stronger departure from the classical scaling through

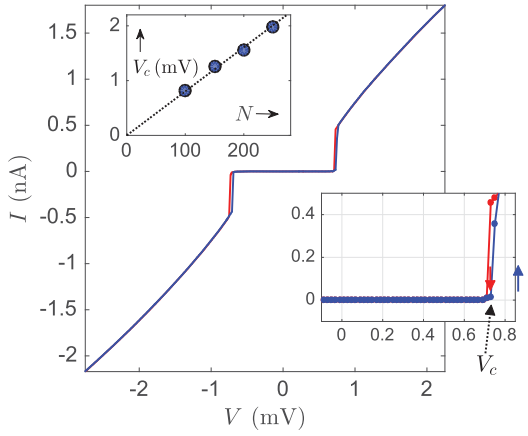

FIG. 2. (Main plot) Experimental determination of the critical voltage for a $N = 250$, family 1, device CS3 (see SM [26]). The blue data are obtained upon stepping up from zero voltage, and the red when stepping back down from nonzero current. (Lower inset) Closeup of the small voltage region where the critical voltage is extracted. A very small hysteresis region is present in the IVC for this device. The critical voltage is taken to be the average value of the switching voltage, where the latter is defined as the voltage having maximum dI/dV upon stepping up from zero voltage. (Upper inset) Linear dependence of V_c on chain length, N, for a family of devices where only length has been varied.

Eq. (4), as one moves closer to the SF-BG quantum phase transition at $K_c = 3/2$.

In Fig. 3, we plot the dimensionless scaled critical voltage, v, as a function of the scaled, single-junction Bloch bandwidth, $w = W/\hbar\omega_p$. W has been calculated by numerical diagonalization of the Hamiltonian for a single, current-biased junction, using the experimentally determined values of E_J and E_{CP} for each device. The blue and black dotted lines are the classical expression of the depinning theory, Eq. (3) [22], for differing Λ, which are already substantially reduced from the red solid line that arises from a model based on independent, coherent QPS (rigid quasicharge, i.e., infinite screening length).

For Fig. 3, we performed a least-squares fit to screening length Λ and prefactor b, using the disordered LL theory, resulting in the solid blue and black lines for devices without and with ground planes, respectively. Note that K is determined from independent measurement of E_J and E_{CP}, combined with fit values of the screening length Λ (or alternatively E_0). The fitted values of screening length are $\Lambda = 13.1$ for devices without ground planes, and $\Lambda = 4.0$ for the devices with ground plane. The fitted prefactor for devices without ground planes is 11% larger than the classical value found by Fukuyama and Lee in the context of charge density waves [16]; however, for ground plane devices it is 28% smaller. Corrections to the theory arising from slightly nonmaximal charge disorder or other microscopic assumptions, would result in a modified prefactor.

For comparison, we have also included in Fig. 3 the disordered LL theory using the Fukuyama-Lee prefactors

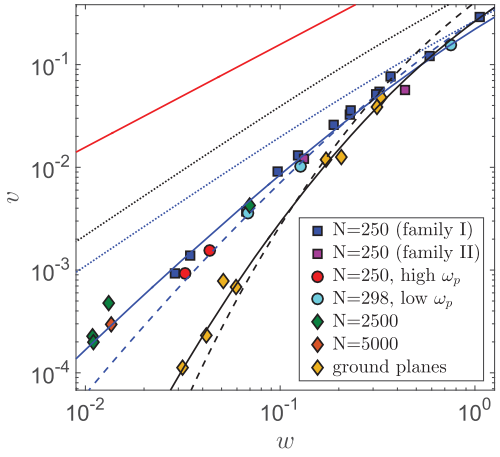

FIG. 3. Scaled critical voltage $v = eV_c/N\hbar\omega_p$, versus scaled Bloch bandwidth $w = W/\hbar\omega_p$. Symbols represent different fabrication "families" distinguished by plasma frequency ω_p, length, and presence of ground plane (see SM [26]). The solid red line is theory for independent QPS across each junction (additive Coulomb blockade, or "rigid" quasicharge, and no disorder) and has slope = 1. Solid lines are the quantum theory of a disordered Luttinger mode, Eq. (4), with fitted values of screening length $\Lambda = 13.1$ (blue), and $\Lambda = 4.0$ (black), respectively. These exhibit a w-dependent slope, $4/(3-2K)$, where $K(w)$ is the Luttinger parameter. For small w, $K \propto \Lambda^{-1} \ln w$: for the same range of w, K is enhanced by the decreased screening length of devices with ground planes, resulting in a stronger departure from the classical result. The dotted lines show the classical depinning result, slope $= 4/3$, for $\Lambda = 13.1$ (dotted blue) and $\Lambda = 4.0$ (dotted black). Also plotted for comparison are the quantum results for $\Lambda = 7.7$ (blue dashed), and $\Lambda = 3.2$ (black dashed), screening lengths inferred from the gate-dependent periodicity of dI/dV at large w and biases $V > V_c$ (see SM [26]).

(dashed blue and black lines), combined with values of Λ determined from the observed periodicity in gate voltage, ΔU, of the conductance (see SM [26]). Here one assumes the observed period in the normal state is given by $\Delta U C_0 = e$; however, additional theory is necessary to understand the experimentally observed periodicities in the transport regime. This approach, which involves no fitting parameters, nevertheless is a very good match to the data, in contrast to the classical result.

For small w, $K \propto \Lambda^{-1} \ln w$, explicitly showing that over the same range of w, K is enhanced by the decreased screening length of devices with ground planes, resulting in a stronger departure from the classical result.

We conclude that the data are clearly inconsistent with the classical depinning theory (slope $4/3$), but can be accurately described by the quantum theory, which includes steepening of the localization length exponent with Luttinger parameter K. Note that according to theory, reducing the screening length pushes the classical theory ($K = 0$) to higher scaled critical voltages (dotted black line compared to dotted blue), in opposition to the quantum result, which is in excellent agreement with our experiments where we have systematically increased K by reducing the screening length using ground planes.

The universal scaling of the data is furthermore notable as it covers 3 orders of magnitude in v, 2 in w, nearly 2 in length ($N = 100$–5000), and greater than 1 in plasma frequency. We therefore identify and demonstrate quantitatively a unique signature of the Bose glass in Josephson-junction chains, as a precursor to Bose-glass-to-superfluid transition at $K_c = 3/2$, and confirm the quantum theory of disordered one-dimensional bosonic insulators based on an interacting Luttinger-liquid picture.

Based on a finite size analysis of the zero-bias resistance of SQUID chains, the authors of Ref. [8] concluded that the one-dimensional superfluid-insulator transition occurs at an anomalously low value for the Luttinger parameter [31,32]. In view of our single-junction chain results, which are in remarkable quantitative agreement with theory of the superfluid-Bose glass transition, there appears to be a discrepancy. We have recently measured SQUID chains that indeed show significantly reduced critical voltages compared to our single-junction chains [33]. Additional experimental work is needed to resolve the matter, which could indicate a nontrivial interplay of flux and charge in SQUID chains.

In the BH model, a sequence of Mott lobes occurs with variation of the chemical potential μ. With disorder in μ, a Bose glass phase intervenes between Mott insulator and superfluid phases [3]. For sufficiently strong disorder, the Mott lobes disappear, leaving only the Bose glass. For our devices, the chemical potential is related to gate voltage U. We have found no appreciable gate dependence of V_c in any device. This can be understood as a consequence of maximal offset charge disorder, and indicative of the possible ubiquity of the Bose glass phase in insulating Josephson-junction arrays.

Given that materials used for quantum phase slip devices are significantly disordered, we believe it likely that the Bose glass behavior we have found in JJ chains may well extend to such superconducting nanowires. In contrast to the rigid Mott insulator, the Bose glass has nonzero compressibility due to low-energy rearrangements of domain boundaries. In JJ chains, these are Cooper pairs (or Cooper-pair holes), localized over the pinning length, N_L. Their number and configuration are randomly changed by external voltages. We argue that this could explain the lack of success in achieving sharp current steps under rf or microwave driving, for both junction chains [34] and superconducting nanowires [35,36].

This work was supported by the Centre of Excellence for Engineered Quantum Systems, an Australian Research Council Centre of Excellence, Grant No. CE110001013. Devices were fabricated at the UNSW Node of the Australian National Fabrication Facility. A. S. was

supported by the Russian Science Foundation (Grant No. 14-42-00044). N. V. was supported by Australian Research Council under the Discovery Grant No. DP140100375, with computational resources provided by the NCI National Facility systems at the Australian National University through the National Computational Merit Allocation Scheme supported by the Australian Government. A. S. thanks D. G. Polyakov for useful discussions.

*Present address: Physics Department, Lancaster University, Lancaster LA1 4YB, United Kingdom.
†To whom correspondence should be addressed. t.duty@unsw.edu.au

[1] D. Jaksch, C. Bruder, J. I. Cirac, C. W. Gardiner, and P. Zoller, Phys. Rev. Lett. **81**, 3108 (1998).
[2] M. Greiner, O. Mandel, T. Esslinger, T. W. Hänsch, and I. Bloch, Nature (London) **415**, 39 (2002).
[3] M. P. A. Fisher, P. B. Weichman, G. Grinstein, and D. S. Fisher, Phys. Rev. B **40**, 546 (1989).
[4] T. Giamarchi and H. J. Schulz, Phys. Rev. B **37**, 325 (1988).
[5] T. Giamarchi, *Quantum Physics in One Dimension* (Clarendon Press, Oxford, 2003).
[6] R. M. Bradley and S. Doniach, Phys. Rev. B **30**, 1138 (1984).
[7] L. J. Geerligs, M. Peters, L. E. M. de Groot, A. Verbruggen, and J. E. Mooij, Phys. Rev. Lett. **63**, 326 (1989).
[8] E. Chow, P. Delsing, and D. B. Haviland, Phys. Rev. Lett. **81**, 204 (1998).
[9] A. D. Zaikin, D. S. Golubev, A. van Otterlo, and G. T. Zimányi, Phys. Rev. Lett. **78**, 1552 (1997).
[10] I. M. Pop, I. Protopopov, F. Lecocq, Z. Peng, B. Pannetier, O. Buisson, and W. Guichard, Nat. Phys. **6**, 589 (2010).
[11] W. Guichard and F. W. J. Hekking, Phys. Rev. B **81**, 064508 (2010).
[12] J. E. Mooij and Y. V. Nazarov, Nat. Phys. **2**, 169 (2006).
[13] D. Haviland, Nat. Phys. **6**, 565 (2010).
[14] G. Rastelli, I. M. Pop, and F. W. J. Hekking, Phys. Rev. B **87**, 174513 (2013).
[15] A. Ergül, J. Lidmar, J. Johansson, and Y. Azizoğlu, D. Schaeffer, and D. B. Haviland, New J. Phys. **15**, 095014 (2013).
[16] H. Fukuyama and P. A. Lee, Phys. Rev. B **17**, 535 (1978).
[17] A. I. Larkin and Y. N. Ovchinnikov, J. Low Temp. Phys. **34**, 409 (1979).
[18] Y. Imry and S. Ma, Phys. Rev. Lett. **35**, 1399 (1975).
[19] Y. Suzumura and H. Fukuyama, J. Phys. Soc. Jpn. **52**, 2870 (1983).
[20] Quasicharge is well known in the theory of Coulomb blockade and appears naturally in the theories including a phenomenological inductance. It is seen to be analogous to quasimomentum that arises in the quantum theory of a particle in a periodic potential; see [21].
[21] K. K. Likharev and A. B. Zorin, J. Low Temp. Phys. **59**, 347 (1985).
[22] N. Vogt, R. Schäfer, H. Rotzinger, W. Cui, A. Fiebig, A. Shnirman, and A. V. Ustinov, Phys. Rev. B **92**, 045435 (2015).
[23] V. Gurarie and A. M. Tsvelik, J. Low Temp. Phys. **135**, 245 (2004).
[24] D. B. Haviland and P. Delsing, Phys. Rev. B **54**, R6857 (1996).
[25] S. Brazovskii and T. Nattermann, Adv. Phys. **53**, 177 (2004).
[26] See Supplemental Material http://link.aps.org/supplemental/10.1103/PhysRevLett.119.167701 for a description of sample fabrication, microwave filtering, and how E_J, E_{CP}, V_c, and C_0 have been determined from the experimental data. Supplemental Material includes Refs. [27–30].
[27] T. S. Tighe, M. T. Tuominen, J. M. Hergenrother, and M. Tinkham, Phys. Rev. B **47**, 1145 (1993).
[28] K. Cedergren, S. Kafanov, J.-L. Smirr, J. H. Cole, and T. Duty, Phys. Rev. B **92**, 104513 (2015).
[29] L. S. Kuzmin, P. Delsing, T. Claeson, and K. K. Likharev, Phys. Rev. Lett. **62**, 2539 (1989).
[30] P. Delsing, in *Single Charge Tunneling*, edited by H. Grabert and M. H. Devoret (Plenum, New York, 1992), pp. 249–274.
[31] D. B. Haviland, K. Andersson, P. Ågren, J. Johansson, V. Schöllmann, and M. Watanabe, Physica (Amsterdam) **352C**, 55 (2001).
[32] M.-S. Choi, M. Y. Choi, T. Choi, and S.-I. Lee, Phys. Rev. Lett. **81**, 4240 (1998).
[33] K. Cedergren, R. Ackroyd, T. Faros, and T. Duty (to be published).
[34] K. Andersson, P. Delsing, and D. Haviland, Physica (Amsterdam) **284–288B**, 1816 (2000).
[35] C. N. Lau, N. Markovic, M. Bockrath, A. Bezryadin, and M. Tinkham, Phys. Rev. Lett. **87**, 217003 (2001).
[36] J. S. Lehtinen, K. Zakharov, and K. Yu. Arutyunov, Phys. Rev. Lett. **109**, 187001 (2012).